ELSEVIER

Biophysical Chemistry 94 (2001) 107–120

Biophysical Chemistry

www.elsevier.com/locate/bpc

Evidence of reduced flexibility in disulfide bridge-depleted azurin: a molecular dynamics simulation study

Bruno Rizzuti, Luigi Sportelli, Rita Guzzi*

Dipartimento di Fisica e Unità INFM, Laboratorio di Biofisica Molecolare, Università della Calabria, Ponte P. Bucci, Cubo 30C, 87030 Rende (CS), Italy

Received 15 May 2001; received in revised form 3 September 2001; accepted 6 September 2001

Abstract

Two molecular dynamics simulations have been performed for 2 ns, at room temperature, on fully hydrated wild type and Cys3Ala/Cys26Ala double-mutant azurin, to investigate the role of the unique disulfide bridge on the structure and dynamics of the protein. The results show that the removal of the −SS− bond does not affect the structural features of the protein, whereas alterations of the dynamical properties are observed. The root mean square fluctuations of the atomic positions are, on average, considerably reduced in the azurin mutant with respect to the wild type form. The number of intramolecular hydrogen bonds between protein backbone atoms that are lost during the simulation, with respect to the starting configuration, are reduced in the absence of the disulfide bond. The analysis of the dynamical cross-correlation map, characterising the protein co-ordinated internal motions, demonstrates in the mutated azurin a significant decrease in anti-correlated displacements between protein residues, with the only exception occurring in the region of the mutation sites. The overall findings show a relevant reduction in flexibility as a consequence of the disulfide bridge depletion in azurin, suggesting that the −SS− bond is a structural element which significantly contributes to the dynamic properties of the native protein.

Keywords: Azurin; Molecular dynamics simulation; Disulfide bridge; Flexibility

* Corresponding author. Tel.: +39-0984-496077; fax: +39-0984-494401.
E-mail address: guzzi@fis.unical.it (R. Guzzi).

0301-4622/01/$ - see front matter
PII: S0301-4622(01)00228-9

1. Introduction

It is well established that proteins are flexible molecules, requiring internal motion to perform their biological function. The dynamic properties of a polypeptide chain depend upon its conformation, which in turn is determined by the different interactions involving every single amino acid residue [1]. Disulfide bridges are the only covalent bonds that residues further along the primary structure can form, and therefore their presence represents a strong constraint on the molecular structure. A possible role of the disulfide bridges has been suggested and it consists of reducing the number of conformations that the polypeptide chain can assume in the folded state [2,3]. This stabilising mechanism acts during the folding process, but once the native structure is reached, it can be hypothesised that –SS– bonds contribute in determining the dynamic features of the protein. In this respect, however, the role of these bonds is not yet well established. In the investigation of this aspect, it has to be taken into account that a disulfide bridge should not be considered as a separate element with respect to the global protein system. In fact, although the –SS– constraint has a local character, its effects must be regarded in a more general context, influencing the dynamics of the whole molecular structure specifically investigated.

Azurin is a blue copper protein belonging to the cupredoxins family, acting as an electron transfer shuttle in the redox system of *Pseudomonas aeruginosa* and some other bacteria, and bear-

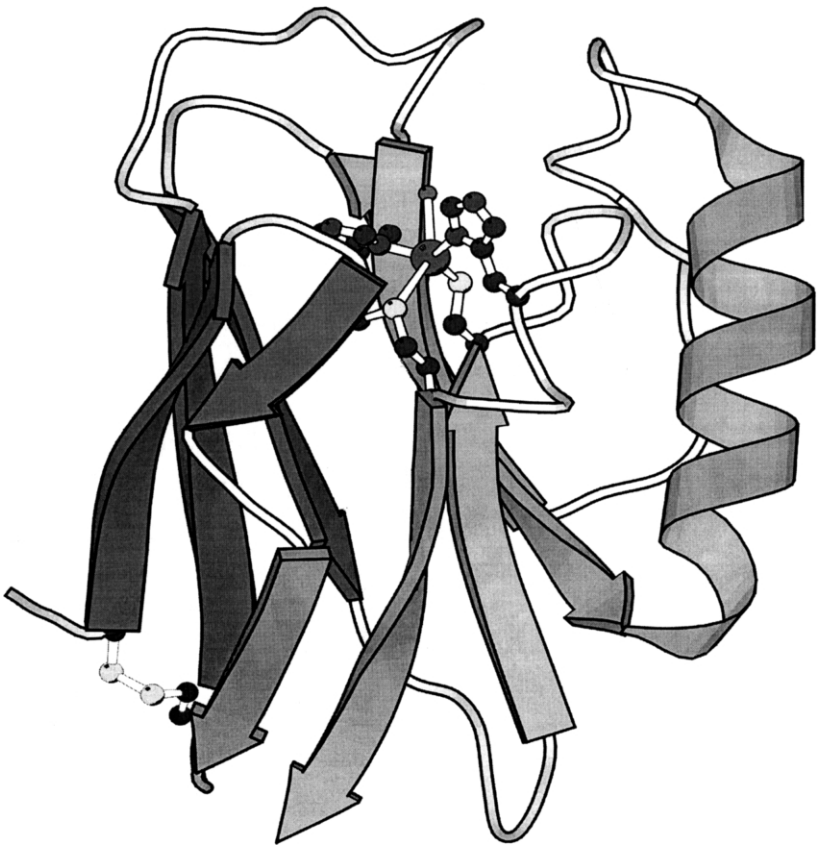

Fig. 1. Model of native azurin, generated with MOLSCRIPT program [31]. The copper ion with its ligands (top) and the disulfide bridge (bottom) are shown.

ing a unique disulfide bridge. The native protein is formed by 128 amino acids, with the −SS− bond connecting cysteine residues 3 and 26. The tertiary structure is dominated by two face-to-face β-sheets arranged in a Greek key folding motif, conventionally represented as in Fig. 1. In the active site, a copper (Cu) ion is sandwiched between the two β-sheets, approximately 0.7 nm below the protein surface; the five Cu−ligand residues are Gly45, His46, Cys112, His117 and Met121. The secondary structure of wild-type (azurin), obtained by X-ray diffraction [4], demonstrates that the two β-sheets are formed by eight strands numbered from S1 to S8, as indicated in Fig. 2. Due to its high β-structure content, azurin should be considered a prevalently rigid, high

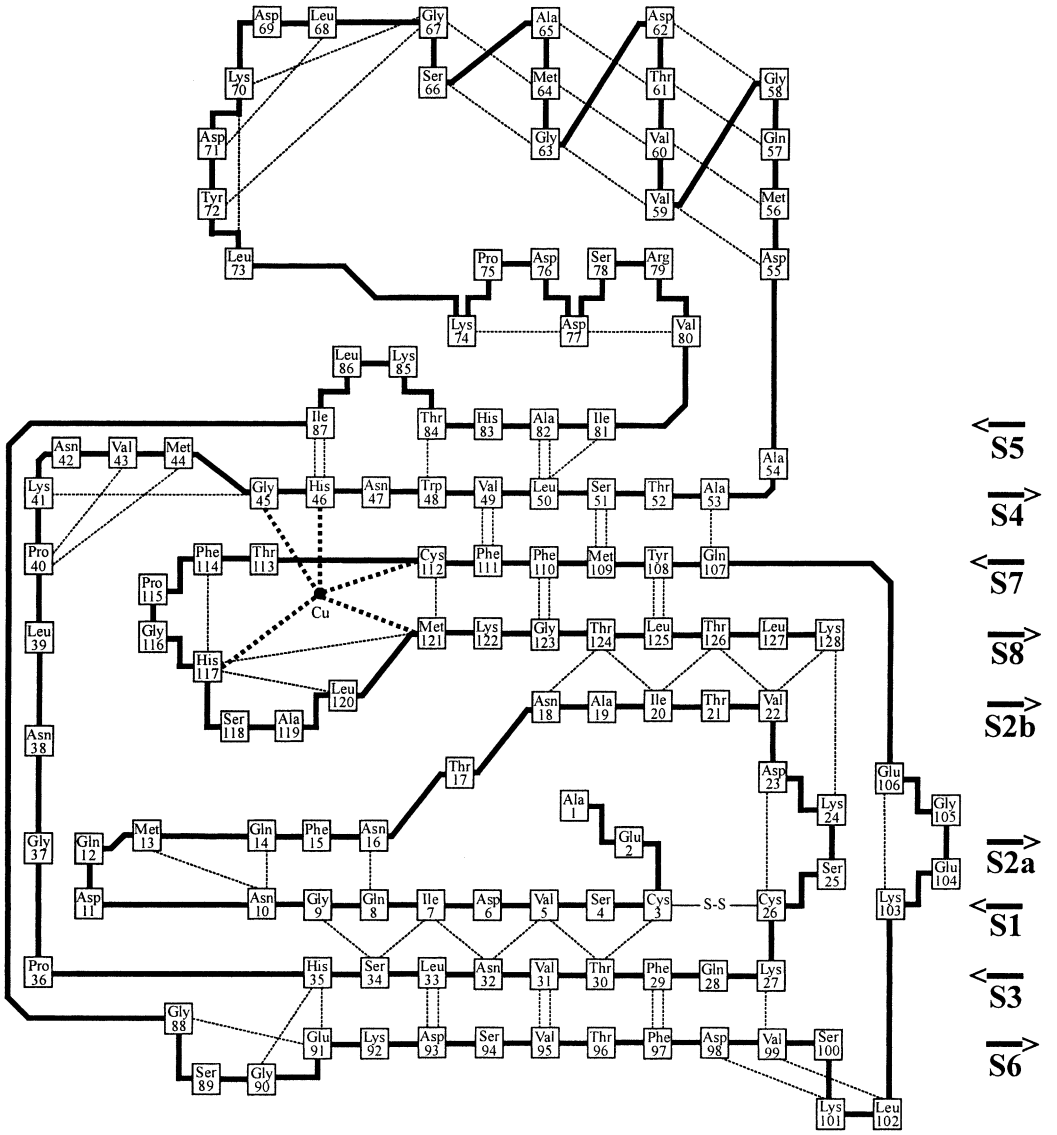

Fig. 2. Diagram of the hydrogen bond patterns for the crystal structure of native azurin [4]. Backbone covalent bonds (strong solid line), copper ion−ligand interactions (strong dashed line), hydrogen bonds (thin dashed line) and the disulfide bridge between Cys3 and Cys26 residues are shown. The S1–S8 strands are also indicated.

co-operative structure. A helix followed by a coil region is also present, approximately on the opposite side with respect to the disulfide bridge.

Crystallographic, kinetic and spectroscopic studies carried out in recent years have well characterised azurin in wild type and numerous mutated forms, providing important structural and dynamic information. In particular, the mutated azurin that we are interested in is the –SS–-depleted form obtained by replacing both Cys with Ala residues [5,6]. Experimental results show that this mutation, although not altering the overall structure of the protein, significantly affects the thermodynamic stability of the molecule. In fact, the denaturation temperature is reduced by approximately 20 K and the Gibbs free energy value is half that of the native form [5]. Experimental techniques, however, typically supply data that are averaged over a wide time range. Moreover, the dynamic behaviour of the protein structure cannot be observed on the overall molecule in its atomic details. Thus, molecular dynamics simulations (MDS) are useful tools to better elucidate these aspects on a time scale up to nanoseconds.

In this work, MDS has been used to study the role of the disulfide bridge on the structure and dynamics of *Pseudomonas aeruginosa* azurin. The results obtained show that the structural features of wild type (Wt) and Cys3Ala/Cys26Ala double-mutant (Dm) azurin are very similar. On the contrary, the dynamic behaviour of the two proteins is rather different, and indicates a higher stiffness of azurin in absence of the disulfide bridge. Experimental results obtained by some of us, concerning a reduction in the width of the conformational substates distribution in the Dm mutant with respect to the Wt protein [7], indirectly confirm this rather surprising finding. We suggest that a possible role of the disulfide bridge in Wt azurin might be to maintain the flexibility of the whole molecule.

2. Computational methods

2.1. Molecular modelling and dynamics

MDS of Wt and Dm azurins were performed under the same conditions using the GROMOS96 package [8]. The starting structure of azurin was taken from the 4AZU entry of the Protein Data Bank, containing the X-ray co-ordinates of oxidised *Pseudomonas aeruginosa* azurin at pH 5.5, resolved at 0.19 nm in a tetramer unit [4]. Only one monomer of the tetramer was considered, together with its related crystallisation waters. The atomic charge value of all the ionisible residues was assumed to be appropriate to pH 7.0. The disulfide bridge in the Wt protein has been explicitly indicated, whereas the connected S atoms of cysteine residues 3 and 26 have been eliminated in the Dm protein, and an extra H atom has been added to both C atoms at position β of the residues. Experimental results indicate that such an alteration, corresponding to a Cys into Ala residue mutation, does not affect the correct folding of the protein structure [5,6].

The Cu atom in azurin is co-ordinated to three equatorial ligands, namely the $N^{\delta 1}$ atoms of His46 and His117 and the S atom of Cys112. Two additional axial ligands are the S atom of Met121 and the carbonyl O of Gly45 [4]. Each Cu–ligand interaction has been taken into account by covalent bonds, on the grounds of experimental evidence [9]. The overall charge of the Cys112 residue was set to $-0.5e$, whereas the other four ligand residues were considered neutral. A charge of $+0.5e$ was given to the Cu ion, to obtain a global null net charge for the active site. Each protein molecule was centred in a regular, truncated octahedron box corresponding to a cube of edge length 6.507 nm, filled with bulk SPC/E water molecules [10]. Solvent molecules placed at a distance from any protein atom smaller than 0.23 nm were removed to give a final, fully hydrated system containing 3980 water molecules, corresponding to 5 g water/g protein. Periodic boundary conditions were applied to avoid edge effects.

A cut-off radius of 0.8 nm for non-bonded interactions and of 1.4 nm for long-range electrostatic interactions was used [11], with an update of the neighbours pair list every 10 steps. A Poisson–Boltzmann reaction field was employed to take into account the electrostatic interactions beyond the long-range cut-off radius. The tem-

perature of both protein and solvent was separately coupled to an external bath with relaxation times of 0.1 ps. An energy minimisation using the steepest descent method was performed for 116 steps, to relax the system and avoid poor contacts. During minimisation, a harmonic position restraining with a force constant of 9000 kJ mol^{-1} nm^{-2} was used to minimise the protein atomic deviations from the crystal structure. The Shake constraint algorithm [12] was used to fix the bond length of protein and water molecules at their equilibrium values within a relative tolerance of 10^{-4}.

Initial atomic velocities were assigned from a Maxwellian distribution corresponding to a starting temperature of 250 K [13]. A time step of 0.002 ps was used for integrating the equations of motion. The system was thermalised for 50 ps by increasing the temperature from 250 to 300 K every 2 ps, and a positional restraining force with a constant decrease from 9000 to 50 kJ mol^{-1} nm^{-2} was also applied. The simulations were performed at constant volume for 2000 ps, saving the configurations of trajectories and energy every 0.1 ps.

2.2. Data analysis procedures

A number of properties were monitored to check the time evolution of the simulation process for both Wt and Dm azurin. The potential and kinetic total energy of the system show an increase during the thermalisation phase, and relatively short period oscillations after 50 ps (data not shown). The gyration radius for both proteins shows a small fluctuation around the starting value of 1.39 nm (data not shown), assuring that the molecules preserve a folded structure during the simulation. The root mean square deviations (RMSD) of the protein atomic positions demonstrate an initial rise during an equilibration period of 100 ps, followed by relatively short-term oscillations (data not shown). Therefore, only the 100–2000-ps time interval has been considered for the analysis of structural and dynamic properties of azurin; this data-analysis time interval is hereafter referred to as the simulation time.

To study the mobility of the protein structural elements, deviations of the atomic positions from the crystallographic configuration were valued as a function of the residue number. The overall translational and rotational molecular motion was removed by superimposing the protein main chain at each time step onto the reference structure backbone, by mean of a mass-weighted least-square algorithm [14]. The RMSD of atomic positions of both the backbone and side chains were then calculated for any protein residue according to the expression:

$$\Delta R = \left(\frac{1}{N} \sum_{i=1}^{N} \langle \Delta r_i^2 \rangle \right)^{1/2} \quad (1)$$

where N is the number of atoms, Δr_i is the difference between the instantaneous and starting position for the ith atom, and the angular brackets indicate a time average over the simulation time.

The same procedure and expression have been used to compute the root mean square fluctuations (RMSF) of atomic positions as a function of the residue number. In this case, ΔR represents the RMSF of a given residue, whereas Δr_i is the difference between the instantaneous and averaged position of the ith atom.

The RMSF have been compared with the same values derived from the B-factors of the crystallographic Wt azurin structure, calculated for every residue according to the expression [15]:

$$\Delta R_{\mathrm{F}} = \left(\frac{3\mathrm{B}}{8\pi^2} \right)^{1/2} \quad (2)$$

A geometric criterion has been used to define the formation of a hydrogen bond (HB) during the simulation, requiring a hydrogen–acceptor distance shorter then 0.32 nm and a donor–hydrogen–acceptor angle larger than 120° [16]. The bond is assumed to exist if it is present for more than 25% of the simulation time.

To analyse the collective motions of the amino acid residues, a dynamical cross-correlation map (DCCM) was used. Correlated motion between the ith and jth residues, with $i \leq j$, is described by a coefficient C_{ij}, given by [17]:

$$C_{ij} = \frac{\langle r_i r_j \rangle - \langle r_i \rangle - \langle r_j \rangle}{\left[\left(\langle r_i^2 \rangle - \langle r_i \rangle^2\right)\left(\langle r_j^2 \rangle - \langle r_j \rangle^2\right)\right]^{1/2}} \quad (3)$$

The value of C_{ij} ranges between -1 and 1. Negative values are indicative of displacements along opposite directions, namely anticorrelated motions, whereas positive values are indicative of properly correlated motions occurring along the same direction. The DCCM is a square matrix built using the C_{ij} values. If C_{ij} has a positive value, the same value is given to the (i,j) element of the matrix, whereas the symmetric (j,i) element is set to zero. On the contrary, if C_{ij} has a negative value, the same value is given to the (j,i) element of the matrix and the (i,j) element is set to zero.

3. Results and discussion

3.1. Structure mobility

Conformational changes in protein structure during the simulation can be demonstrated by the analysis of the time-averaged simulated deviations from the starting configuration, as a function of the residue number. The RMSD of the backbone atoms, N–C^{α}–CO, are reported in Fig. 3 for both Wt (solid line) and Dm protein (dashed line). In general, the values registered for the deviations are quite small compared with those found in MDS of other proteins [18]. The mean values are below 0.09 nm and no maximum is above 0.25 nm, which is consistent with the structural features of azurin, mainly a beta-type protein. The lowest RMSD values are found for the regions most structurally organised, for example corresponding to the helix and the Cu–ligand residues. On the contrary, high RMSD values are generally found for secondary structure elements, such as turns and loops, that are also more exposed to the solvent.

The analysis of the RMSD for the Wt protein (Fig. 3, solid line) shows an absolute maximum for the Gly105 residue, which can be interpreted in terms of the mobility shown by the turn, including residues 103–106. On the whole, however, the

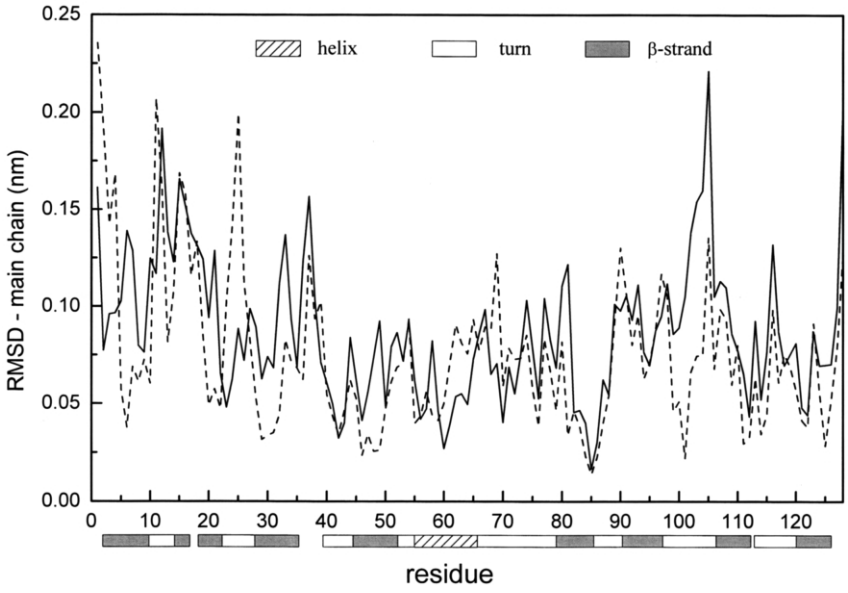

Fig. 3. Root mean square deviations (RMSD) between the crystal structure and the conformation obtained from simulation data, averaged over the 100–2000-ps time interval and plotted vs. backbone N–C^{α}–CO atoms, for both wild type (solid line) and Cys3Ala/Cys26Ala double-mutant (dashed line) azurin. Secondary structural elements are also shown.

greatest deviations are found in the region including residues 7–16, in the S1–S2a strands interface (Fig. 2). Furthermore, backbone atomic deviations are found for residues 32–34, belonging to the S3 strand located in front of the central part of the S1 strand. This finding gives a first indication of a reorganisation of the interface between the S1–S2a strands. Other regions showing significant deviations in the Wt azurin are the Pro36–Pro40 loop and both ends of the main chain. In particular, the C-terminus shows a RMSD value higher than the N-terminus, which is partially constrained by the disulfide bridge that restricts the motion of the Cys3 residue.

When compared, the RMSD of Dm azurin (Fig. 3, dashed line) are generally similar to the Wt protein values, both qualitatively and quantitatively. The most evident differences are found corresponding to the mutation sites, at position 3 and 26. Both the N-terminus and the Asp23–Ala26 turn in the Dm azurin are no longer constrained by the disulfide bridge, so that they show high deviation values. Further differences, directly ascribable to the local rearrangement occurring within the mutation sites, are registered corresponding to the S1 strand and the central part of the S2a and S2b strands, in this case producing lower RMSD compared to the Wt protein. The same is observed in the central part of the S1 strand, which consequently reflects on residues 32–34 in the S3 strand.

Differences between the RMSD values of Wt and Dm azurin are also evident for the other structural elements that are close to the –SS– bond in the tertiary structure of the native protein (Fig. 1), namely the C-terminus and the coil region including the 103–106 turn. However, in this case, atomic deviations in the Dm structure are much smaller than in the Wt protein. Similar behaviour is registered for the Trp48 residue, suggesting that in the Dm azurin, the hydrophobic core may be more constrained with respect to the native form.

For both Wt and Dm proteins, side chain deviations essentially confirm all the indications given by the backbone RMSD plot, although the values are generally greater because of their higher mobility (data not shown).

3.2. Wild type azurin flexibility

The extent of protein motion during the simulation time characterises the flexibility of the macromolecule structure. Fig. 4 shows the RMSF of Wt (solid line) and Dm (dashed line) azurin main-chain atoms as a function of the residue number, together with the same values derived from the crystallographic B factors of the Wt protein (dotted line).

The backbone RMSF values of Wt azurin show a mean value of 0.070 nm. The RMSF of the Cu ligands are nearly identical to the crystallographic values, indicating a significant rigidity of the active site. This feature, which is widely documented, is believed to be essential for high efficiency of the electron transfer process [19]. The central region of every β-strand, generally involving no more than two or three residues, is characterised by fluctuations lower than the corresponding B-factors, the minimum value corresponding to the Trp48 residue buried in the protein core. Hence, the dynamics of these regions appears to be highly hindered by the overall β-sheet scaffold stiffness.

The RMSF values found by simulation are also lower than in the crystal for a long portion of the main chain between residues 58 and 78, including the terminal part of the helix and the coil connecting it to the following β-strand. In order to explain this result, it should be remarked that experimental RMSF values derived from X-ray data are essentially due to thermal fluctuations, conformational disorder and crystal distortions of the protein structure. Likewise, simulation data contain information about thermal disorder, but also on conformational substate distribution. In fact, if the simulation time is longer than the relaxation time of a physical parameter of interest, an average obtained on an equilibrium trajectory can reliably approximate the value achievable with a measurement of virtually infinite duration [20]. Furthermore, according to the ergodic hypothesis, this time average is equivalent to an ensemble average. This implies that time-mediated quantities, such as RMSF, can be assumed to be representative of a sufficient number of en-

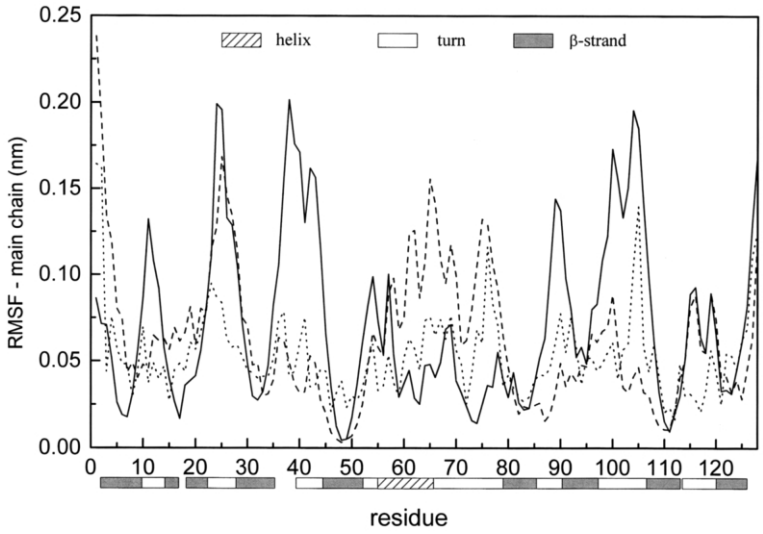

Fig. 4. Root mean square fluctuations (RMSF) obtained from simulation data, averaged over the 100–2000-ps time interval and plotted vs. backbone N–C^{α}–CO atoms, of both wild type (solid line) and Cys3Ala/Cys26Ala double-mutant (dashed line) azurin. The same value obtained from the crystallographic B-factors (dotted line) is reported. Secondary structural elements are also shown.

semble members, even if extrapolated from a single macromolecule simulation. Owing to the equilibration period, fluctuations calculated from a MDS are only slightly influenced by crystal distortion of the starting structure. They are, instead, strongly influenced by the solvent-driven protein internal motion, so that their values are generally higher than the corresponding X-ray value [21]. Therefore, regions where the simulated RMSF are low, as in the terminal region of the helix, may be considered to be affected by a prevalent lattice disorder contribution to the crystallographic fluctuations [22]. This hypothesis is supported by the observation that the crystal unit of azurin is a tetramer, and the helices constitute the main point of contact between the monomers, hence representing an elective under-stress region.

In the complex, the overall stiffness of the protein allows all the RMSF values higher than barely 0.1 nm to be explained in terms of the flexibility shown by specific structural elements. Most of the higher fluctuations are found corresponding to those regions also showing significant deviations. In fact, the turn including residues 103–106 and the main chain C-terminus, exhibiting the two highest RMSD values, are also characterised by some of the highest RMSF values. In both these cases, the simulation data are in agreement with the corresponding crystallographic B-factors, and with NMR measurements performed on Wt azurin in solution [23]. The dynamics of the 103–106 turn possibly also influences the flexibility of the Ser100 residue, located in the same main-chain portion.

Other regions showing high values of both RMSD and RMSF in Wt azurin are the S1–S2a interface, including residues 7–16 and the Pro36–Pro40 loop. In particular, it is interesting to note that the Pro36 residue also shows high fluctuations of the dihedral angles (data not shown). In fact, Pro36 has the maximum value of 50° for both φ and ψ angles, the mean over all the dihedral angles being 15° with a standard deviation of 6°. This suggests that at the pH 7.0 of the simulation, the Pro36–Gly37 peptide bond can easily flip, assuming different conformations without destabilising the overall backbone structure. This finding is experimentally supported by crystallographic data, showing that the pH of the environment determines a local conformational transition of the peptide group at issue [24].

Finally, high flexibility is also found for the two turns including residues 23–26 and 88–91. The former is of particular importance, its dynamics being mainly influenced by the –SS– bond involving the Cys26 residue. In spite of the presence of the disulfide bridge, the 23–26 turn is characterised by flexibility even greater than the N-terminal region, which is analogously restrained by the other end of the bridge. This is surprising, because main chain endings usually have large fluctuations, and could be an indication that the 23–26 turn is involved in determining the flexibility of a region that is important for the dynamic features of Wt azurin.

3.3. Double-mutant azurin flexibility

The RMSF of Dm azurin main-chain atomic positions (Fig. 4, dashed line), compared with the same values derived from the crystallographic B-factors of Wt azurin (dotted line), show that in absence of the disulfide bridge, wide portions of the protein main chain are even less flexible than the Wt structure in the crystal lattice. The simulated RMSF mean value is approximately 15% lower than the corresponding quantity for the Wt protein.

Fluctuations of the Dm protein backbone are higher than the crystallographic values of Wt azurin only corresponding to four definite regions: the Cu-site region between residues 112 and 121, the two mutation sites, and the region including the helix and the turns connecting it to the β-sheets. However, a comparison with simulated Wt azurin RMSF shows that fluctuations in the Cu-site region are very similar in the two proteins. Moreover, the turn including residues 23–26 shows fluctuations comparable with those of the Wt protein, even if no longer constrained by the –SS– bond. This result, together with the difference in the RMSD data of the two simulations, indicates that in the Dm azurin, the region around the mutation site at position 26 undergoes conformational changes rather than increased flexibility. Finally, the RMSF value of residue 3 in the Dm protein is much higher than in the Wt form, but is consistent with the corresponding B-factor value and with the high flexibility generally exhibited by main chain endings. Therefore, the only region showing high flexibility in the Dm protein can be regarded as that furthest away from the mutation sites, corresponding to the helix and the coil backbone portion connecting it to the following β-strand. Increased dynamics of the helical region is clearly evident in the comparison with Wt azurin fluctuations both in crystal and in silico, but also from the typical 'crests' in the RMSF plot, which are representative of residues most exposed to the solvent.

The flexibility of the Dm azurin appears to be dramatically reduced, particularly corresponding to the turns, suggesting that the increase in stiffness of the Dm azurin structure is not uniformly distributed along the protein backbone. On the other hand, an identical minimum of the RMSF is found for both Wt and Dm proteins around the Trp48 residue, indicating that the depletion of the disulfide bridge does not alter the dynamics of the hydrophobic core. More generally, fluctuations in the central part of any β-strand are similar in the two proteins. The only exception is registered in the antiparallel β-loop going from the main chain N-terminus to residue 26. This result suggests that the disulfide bridge contributes to stabilising the S1–S2 strands interface interactions, in agreement with other works [25].

However, it is interesting to observe that the essential structural features of Dm azurin remain unchanged compared to the Wt form, in spite of the considerable differences in the dynamics of the two proteins. Support for this result is given by the analysis of the dihedral angle fluctuations in Dm azurin (data not shown). Even if the positional atomic RMSF values of the Pro36–Pro40 loop show the higher variation compared to the corresponding Wt form ones, in this case the Pro36–Gly37 peptide bond is also free to rotate to assume the appropriate conformation, exactly as observed for the Wt protein.

3.4. Hydrogen bond network analysis

The intramolecular HB network is fundamental

in maintaining the structure of the protein molecule. These bonds are characterised by a relatively low energy, so that they frequently undergo rupture and formation. The analysis of the MDS data reveals that of the 66 HBs between main-chain atoms that exist in the crystallographic configuration, eight are lost during the simulation in the Wt azurin and four in the Dm one. Such a difference between the two proteins is a further indication of greater stiffness of the protein structure in the absence of the disulfide bridge.

Two HBs that are lost only in Wt azurin are those between His35 and Gly90, and Val99 and Leu102. Their rupture can be considered responsible for the high mobility and flexibility values in the corresponding regions of the Wt protein. Similarly, two HBs that are lost in the Dm protein are those between Lys74 and Asp77 and Asp77 and Val80, and their absence can be considered responsible for the high RMSF value in the coil region following the helix. The rupture of the HB between Lys74 and Asp77 also occurs in the Wt protein, and it could explain the fast internal motion of this turn observed by NMR experiments on native azurin in solution, even though on a different time scale [23]. Another bond that is lost in both simulations is that connecting Lys41–Gly45. This HB involves a Cu ligand residue, but it seems of no particular importance, since it is weak even in the starting configuration [4].

Of particular interest is the analysis of the region including residues 7–16, namely the S1–S2a strands interface. In the starting configuration, two HBs between Gln8 and Asn16, and Asn10 and Gln14 connect the two strands, whereas another HB between Asn10 and Met13 is also present. In both simulations, a bond between the amino N atom of Gln8 and the $O^{\delta 1}$ atom of Asn16 replaces the one between the carbonyl O and the amino N of the same residues. The other two HBs are lost only in Wt azurin, and two new intramolecular bonds are registered between the carbonyl O of Glu12 and the amino N of Asn10 and Gln14. The result is that the two strands are interlinked by a HB network reorganisation, yet conserve their face-to-face conformation.

Finally, the last HB which is lost in the Wt azurin simulation is that between Gly63 and Ser66, in the terminal part of the helix, and the consequences of this rupture give rise to the possibility of some considerations. In fact, the azurin helix, including residues 55–67, may not be completely regarded as α-type according to the X-ray data. In the terminal part of the helix, the Asp62 residue does not have a HB partner, and the last two bonds are between Gly63 and Ser66, and Met64 and Gly67, that is an $i \rightarrow i+3$ bond. However, the comparison between crystallographic and simulated fluctuations points to a predominant contribution from lattice disorder in the description of this region obtained by X-ray diffraction. For both Wt and Dm azurin, the MDS data clearly support the indication of a structural rearrangement of this region towards an all-α helix structure in the presence of solvent. In fact, in addition to the breaking of the Gly63–Ser66 bond, two new HBs are formed between Asp62 and Ser66, and Gly63 and Gly67, connecting peptide groups four residues away along the primary structure. Both these bonds are absent in the starting structure, but they are registered afterwards for more than 90% of the MDS time. Differences between a 3^{10} and an α-helix structure are found in the same region comparing the secondary structure obtained by NMR spectroscopy in solution for *Pseudomonas aeruginosa* and *Alcaligenes denitrificans* azurin, which show high homology and an identical HB network organisation [26,27]. This result indicates that the terminal part of the helix region is very sensitive to changes in the surrounding environment.

The formation of a number of new HBs is also observed in some other regions for both proteins, according to other simulation studies [16], but none of these bonds has the property to both alter the secondary structure and show a relevant permanence time. In particular, no intramolecular HB is registered between main-chain atoms of residues belonging to different β-sheets, in agreement with other MDS of cupredoxins [28–30].

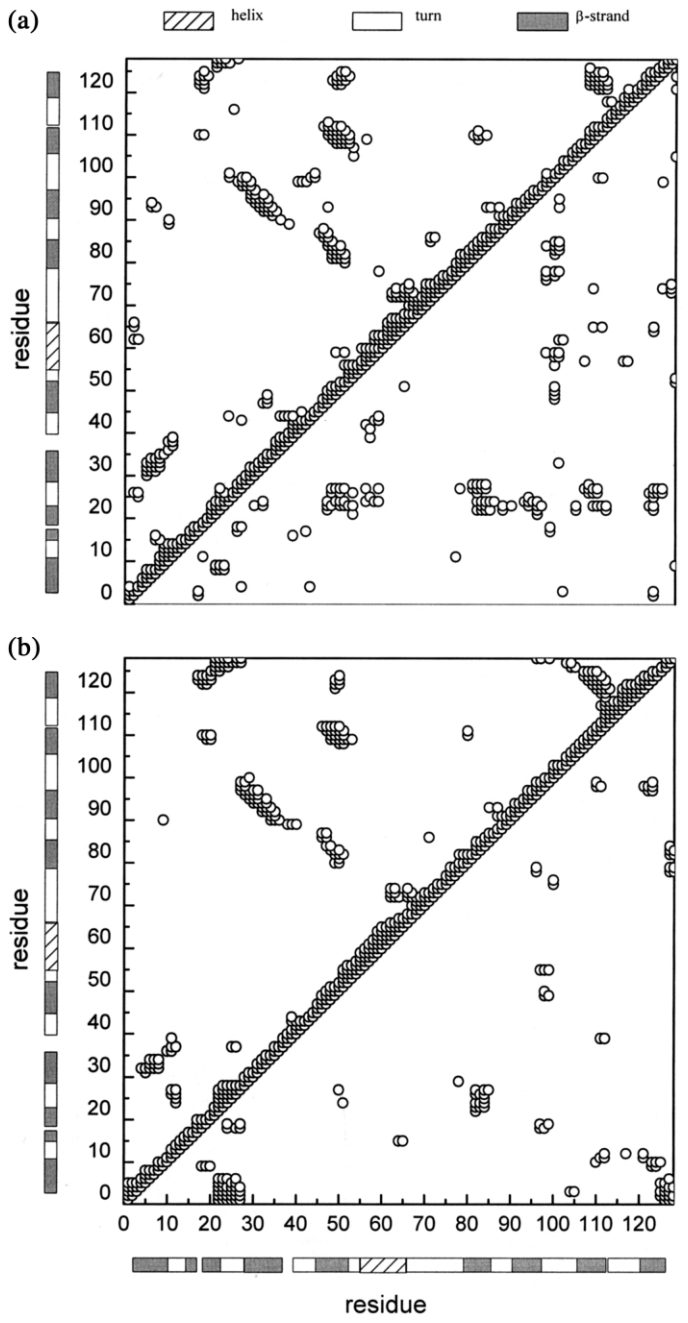

Fig. 5. Dynamical cross-correlation map (DCCM) for the C^{α} atom pairs of both (a) wild type and (b) Cys3Ala/Cys26Ala double-mutant azurin. Only correlation coefficients with an absolute value greater than the threshold value of 0.3 are shown. Positive correlations are mapped in the upper left triangle, negative correlations in the lower right triangle. Secondary structural elements are also shown.

3.5. Cross-correlated motion

The collective character of the motion of the protein residues may reveal important details related to the biological function. The analysis can be performed by means of the DCCM, indicating cross-correlated motion between residues of Wt azurin (Fig. 5a). A threshold value of 0.3 in the module is chosen for the C_{ij} coefficients, which is approximately half the mean value found for the generic ith and $(i+1)$th residues, showing highly correlated motion due to their closeness along the protein primary sequence. Secondary structural elements, such as turns and helices, are determined by interactions involving residues that are near to the primary sequence, so that their correlation is represented by plumes emanating from the main diagonal. For instance, the turn including residues 23–26, the Pro40–Pro44 loop and the region including the helix can be observed.

In the upper left triangle, containing positively correlated motions, the disulfide bridge between Cys3 and Cys26 residues determines the cluster (3,26). Wide clusters are due to co-ordinated movements of faced β-strands. Correlation between antiparallel strands produces clusters perpendicular to the main diagonal, for example the S3–S6, S4–S5 and S4–S7 strands around (32,94), (50,82) and (50,110) respectively. The clusters regarding the S7–S8 and S1–S2a strands are closer to the diagonal, around positions (110,123) and (9,15), respectively. Instead, the cluster (6,32), which is due to the parallel S1–S3 strands, is placed side by side with the main diagonal. Some clusters are also determined by indirect correlations between two β structures. For example, the HB network connecting the S4–S7 and S7–S8 strands generates an indirect correlation between the S4–S8 strands, corresponding to the cluster (50,123).

Correlations between adjacent residues not reciprocally connected by main-chain intramolecular HBs are rare, but not impossible. An example is given by the correlation between residues 63–74 and 71–86, due to the packing of the helix against the β-sheet, and also experimentally observed for both *Pseudomonas aeruginosa* and *Alcaligenes denitrificans* azurins in solution [26,27]. The cluster (85,93) indicates contacts between residues belonging to different β-sheets, again confirmed by experimental evidence [26].

The second half of the DCCM, represented by the lower right triangle below the main diagonal, contains indications about anticorrelated motions between residues. These clusters generally show compensation movements between the two opposite sheets constituting the tertiary structure of azurin. An example is given by the cluster (21,9), generated by negative correlations between the S1–S2b strands. Even if separated by the S2a strand and both positively correlated to it, the S1 and S2b strands belong to different sheets, which tend to mutually equilibrate their motions. This could explain the modifications occurring to the S2a strand, representing a region in which opposite forces come into conflict.

Interesting and numerous anticorrelated motions involve the Asp23 and Cys26 residues, which are directly connected by the HB determining the 23–26 turn. Residues 24–25 are freer in their fluctuations, whereas the motion of both Asp23 and Cys26 is anticorrelated to the region surrounding residues 50, 82, 110 and 123, at the centre of the S4, S5, S7 and S8 strands, and therefore constituting the core region of one of the two β-sheets of azurin.

The analysis of the DCCM of Dm azurin (Fig. 5b) demonstrates a significant reduction in negatively cross-correlated motions between residues with respect to the Wt protein. This result further supports the hypothesis of a higher stiffness of the Dm protein, suggesting a reduced capacity of the structure to adjust its inner motions to the external perturbations in the absence of the disulfide bridge. The structural element most affected is the turn including residues 23–26, which is no longer constrained by the –SS– bond in the Dm protein. It is interesting to note that the only exception to the general trend occurs corresponding to the mutation sites, around position (3,26), where an increase in anti-correlated motions is observed. This behaviour is even more evident as Ala3 and Ala26 are adjacent, along the primary sequence, to residues belonging to the S1 and S3 strands, respectively, which show positively correlated motions.

4. Conclusions

The overall results show that as far as the structural properties are concerned, Wt and Dm azurin are very similar. On the contrary, depletion of the disulfide bridge determines a clear modification of the dynamic properties of the protein. In particular, the modifications found corresponding to the mutation sites are reflected in the S1–S2 β-loop and in the so-called southern pole of azurin. Strong effects are also observed in the helix region, on the opposite side of the mutation sites.

Evidence of greater stiffness of Dm azurin with respect to the Wt form is revealed by analysis of the simulated positional RMSF, and also confirmed by the HB network data and results on cross-correlated displacements. Such findings suggest that the disulfide bridge plays an important role in determining the flexibility features of *Pseudomonas aeruginosa* azurin, possibly acting as a mediator in the redistribution of the dynamics in the molecular structure.

Acknowledgements

B.R. thanks the Regione Calabria for a fellowship. R.G. thanks the INFM, Istituto Nazionale di Fisica della Materia, for a post-doctoral fellowship. Thanks are due to Università della Calabria and INFM for financial support.

References

[1] T.E. Creighton, Protein Folding, W.H. Freeman and Company, New York, 1992.
[2] D.C. Poland, H.A. Scheraga, Statistical mechanics of non-covalent bonds in polyamino acids: covalent loops in proteins, Biopolymers 3 (1965) 373–399.
[3] A.R. Fersht, L. Serrano, Principles of protein stability derived from protein engineering experiments, Curr. Opin. Struct. Biol. 3 (1993) 75–83.
[4] H. Nar, A. Messerschmidt, R. Huber, M. van de Kamp, G.W. Canters, X-Ray crystal structure of the two site-specific mutants His35Gln and His35Leu of azurin from *Pseudomonas aeruginosa*, J. Mol. Biol. 218 (1991) 427–447.
[5] R. Guzzi, L. Sportelli, C. La Rosa, D. Grasso, M.P. Verbeet, G.W. Canters, A spectroscopic and calorimetric investigation on the thermal stability of the Cys3Ala/Cys26Ala azurin mutant, Biophys. J. 77 (1999) 1052–1063.
[6] N. Bonander, J. Leckner, H. Guo, B.G. Karlsson, L. Sjölin, Crystal structure of the disulfide bond-deficient azurin mutant C3A/C26A. How important is the S–S bond for folding and stability? Eur. J. Biochem. 267 (2000) 4511–4519.
[7] R. Guzzi, A. Stirpe, L. Sportelli, Structural heterogeneity of blue copper proteins: an EPR study of amycyanin, wild-type and Cys3Ala/Cys26Ala azurin mutant, Eur. Biophys. J. 30 (2001) 171–178.
[8] W.F. van Gunsteren, F.R. Billeter, A.A. Eising et al., Biomolecular Simulation: The GROMOS96 Manual and User Guide, Vdf Hochschulverlag AG an der ETH Zürich, Zürich, 1996.
[9] H.B. Gray, B.G. Malmström, R.J.P. Williams, Copper co-ordination in blue proteins, J. Biol. Inorg. Chem. 5 (2000) 551–559.
[10] H.J.C. Berendsen, J.R. Grigera, T.P. Straatsma, The missing term in effective pair potentials, J. Phys. Chem. 91 (1987) 6269–6271.
[11] P.J. Steinbach, B.R. Brooks, New spherical cut-off methods for long-range forces in macromolecular simulation, Comp. J. Chem. 15 (1994) 667–683.
[12] J.P. Ryckaert, G. Ciccotti, H.J.C. Berendsen, Numerical integration of the Cartesian equations of motion of a system with constraints: molecular dynamics of n-alkanes, J. Comput. Phys. 23 (1977) 327–341.
[13] H.J.C. Berendsen, J.P.M. Postma, W.F. van Gunsteren, A. Di Nola, J.R. Haak, Molecular dynamics with coupling to an external bath, J. Chem. Phys. 81 (1984) 3684–3690.
[14] R.M. Brunne, K.D. Berndt, P. Guntert, K Wuthrich, W.F. van Gunsteren, Structure and internal dynamics of the bovine pancreatic trypsin inhibitor in aqueous solution from long-time molecular dynamics simulations, Proteins: Struct. Funct. Genet. 23 (1995) 49–62.
[15] A. Kidera, N. Go, Normal mode refinement: crystallographic refinement of protein dynamic structure. I. Theory and test by simulated diffraction data, J. Mol. Biol. 225 (1992) 457–475.
[16] C.A. Schiffer, V. Dötsch, K. Wüthrich, W.F. van Gunsteren, Exploring the role of the solvent in the denaturation of a protein: a molecular dynamics study of the DNA-binding domain of the 434 repressor, Biochemistry 34 (1995) 15057–15067.
[17] P.H. Hünenberger, A.E. Mark, W.F. van Gunsteren, Fluctuations and cross-correlation analysis of protein motion observed in nanosecond molecular dynamics simulations, J. Mol. Biol. 252 (1995) 492–503.
[18] V. Daggett, M. Levitt, Realistic simulations of native-protein dynamics in solution and beyond, Annu. Rev. Biophys. Biomol. Struct. 22 (1993) 353–380.
[19] J.R. Winkler, H.B. Gray, Electron tunneling in proteins: role of the intervening medium, J. Biol. Inorg. Chem. 2 (1997) 399–404.

[20] W.F. van Gunsteren, P.H. Hünenberger, A.E. Mark, P.E. Smith, I.G. Tironi, Computer simulation of protein motion, Comp. Phys. Commun. 91 (1995) 305–319.
[21] G.A. Petsko, D. Ringe, Fluctuations in protein structure from X-ray diffraction, Annu. Rev. Biophys. Bioeng. 13 (1984) 331–371.
[22] E.M. Storch, V. Daggett, Molecular dynamics simulations of cytochrome *b*5: implications for protein–protein recognition, Biochemistry 34 (1995) 9682–9693.
[23] A.P. Kalverda, M. Ubbink, G. Gilardi et al., Backbone dynamics of azurin in solution: slow conformational change associated with deprotonation of histidine 35, Biochemistry 38 (1999) 12690–12697.
[24] H. Nar, A. Messerschmidt, R. Huber, M. van de Kamp, G.W. Canters, Crystal structure analysis of oxidised *Pseudomonas aeruginosa* azurin at pH 5.5 and pH 9.0. A pH-induced conformational transition involves a peptide bond flip, J. Mol. Biol. 221 (1991) 765–772.
[25] N. Bonander, B.G. Karlsson, T. Vänngård, Disruption of the disulfide bridge in azurin from *Pseudomonas aeruginosa*, Biochim. Biophys. Acta 1251 (1995) 48–54.
[26] M. van de Kamp, G.W. Canters, S.S. Wijmenga et al., Complete sequential ^{1}H and ^{15}N nuclear magnetic resonance assignment and solution secondary structure of the blue copper protein azurin from *Pseudomonas aeruginosa*, Biochemistry 31 (1992) 10194–10207.
[27] C.W.G. Hoitink, P.C. Driscoll, H.A.O. Hill, G.W. Canters, ^{1}H and ^{15}N nuclear magnetic resonance assignment, secondary structure in solution, and solvent exchange properties of azurin from *Alcaligenes denitrificans*, Biochemistry 33 (1994) 3560–3571.
[28] A. Ciocchetti, A.R. Bizzarri, S. Cannistraro, Long-term molecular dynamics simulation of copper plastocyanin in water, Biophys. Chem. 69 (1997) 185–198.
[29] C. Arcangeli, A.R. Bizzarri, S. Cannistraro, Long-term dynamics simulation of copper azurin: structure, dynamics and functionality, Biophys. Chem. 78 (1999) 247–257.
[30] R. Guzzi, C. Arcangeli, A.R. Bizzarri, A molecular dynamics simulation study of the solvent isotope effect on copper plastocyanin, Biophys. Chem. 82 (1999) 9–22.
[31] P.J. Kraulis, MOLSCRIPT: a program to produce both detailed and schematic plots of protein structures, J. Appl. Cryst. 24 (1991) 946–950.